IEEE Access
Multidisciplinary ⋮ Rapid Review ⋮ Open Access Journal

Received September 7, 2018, accepted October 2, 2018. Date of publication xxxx 00, 0000, date of current version xxxx 00, 0000.

Digital Object Identifier 10.1109/ACCESS.2018.2874525

Towards Green Energy for Smart Cities: Particle Swarm Optimization Based MPPT Approach

MAJID ABDULLATEEF ABDULLAH[1,2], TAWFIK AL-HADHRAMI[3], CHEE WEI TAN[2], (Senior Member, IEEE), AND ABDUL HALIM YATIM[2], (Senior Member, IEEE)

[1]Faculty of Engineering and Information Technology, Taiz University, Taiz, Yemen
[2]Department of Electrical Power Engineering, Faculty of Engineering, School of Electrical Engineering, Universiti Teknologi Malaysia, Johor Bahru, Malaysia
[3]School of Science and Technology, Nottingham Trent University, Nottingham, U.K.

Corresponding authors: Majid A. Abdullah (aaamajid2@gmail.com) and Tawfik Al-Hadhrami (tawfik.al-hadhrami@ntu.ac.uk)

This work was supported in part by Universiti Teknologi Malaysia, Power Electronics and Drives Research Group and in part by Nottingham Trent University, Network Infrastructures and Cyber Security Group.

ABSTRACT This paper proposes an improved one-power-point (OPP) maximum power point tracking (MPPT) algorithm for wind energy conversion system (WECS) to overcome the problems of the conventional OPP MPPT algorithm, namely, the difficulty in getting a precise value of the optimum coefficient, requiring pre-knowledge of system parameters, and non-uniqueness of the optimum curve. The solution is based on combining the particle swarm optimization (PSO) and optimum-relation-based (ORB) MPPT algorithms. The PSO MPPT algorithm is used to search for the optimum coefficient. Once the optimum coefficient is obtained, the proposed algorithm switches to the ORB MPPT mode of operation. The proposed algorithm neither requires knowledge of system parameters nor mechanical sensors. In addition, it improves the efficiency of the WECS. The proposed algorithm is studied for two different wind speed profiles, and its tracking performance is compared with conventional optimum torque control (OTC) and conventional ORB MPPT algorithms under identical conditions. The improved performance of the algorithm in terms of tracking efficiency is validated through simulation using MATLAB/Simulink. The simulation results confirm that the proposed algorithm has a better performance in terms of tracking efficiency and energy extracted. The tracking efficiency of the PSO-ORB MPPT algorithm could reach up to 99.4% with 1.9% more harvested electrical energy than the conventional OTC and ORB MPPT algorithms. Experiments have been carried out to demonstrate the validity of the proposed MPPT algorithm. The experimental results compare well with system simulation results, and the proposed algorithm performs well, as expected.

INDEX TERMS Wind energy conversion system (WECS), maximum power point tracking (MPPT), particle swarm optimization (PSO), optimum-relation-based (ORB), one-power-point (OPP) MPPT.

I. INTRODUCTION

The world is experiencing a growing population, and in 2050 the population is expected to reach 9 billion [1]. According to some studies [2], [3], about 60% of the population prefer to live in cities. Countries today have an increasing tendency towards smartening of cities [4]–[6]. In a very simple way, a smart city is a sustainable and efficient urban center that provides a high quality of life to its inhabitants through optimal management of its resources [1]. Energy plays a leading role in smart cities, as most of our everyday activities and most of our environment is related to some sort of energy source.

Therefore, in view of the increasing world energy demand, the potential depletion of conventional energy sources, and increasing air pollution due to burning fossil fuels in conventional power plants, renewable energy generators seem as a promising technology for mitigating these challenges. Wind energy is one of the renewable energy sources growing in popularity because of its many advantages such as lower cost of production, sustainability, and being environmentally friendly [7], [8]. It is an endless renewable energy resource and it is expected to be developed as a significant energy source in future [9].

However, based on the Betz limit [10], there is no wind turbine that could convert more than 59.3% of the kinetic energy of the wind into mechanical energy for turning a rotor. The amount of mechanical energy that can be extracted from the wind is governed by the ratio of blade's tip speed (ω_m) to the actual wind speed (V_w). There is a specific ratio for each wind turbine, which is called the optimal tip speed ratio (TSR) or λ_{opt}, at which the extracted power is maximum. Hence, in order to work at this optimal operating point, the wind energy conversion system (WECS) is essential to include an optimization algorithm that can track the maximum peak regardless of wind speed [11]. This optimization algorithm is known as a maximum power point tracking (MPPT) algorithm [8], [12].

In this context, the major contribution of this article is to propose a new and simple MPPT algorithm based on hybridization of the Optimum Relation Based (ORB) and Particle Swarm Optimization (PSO) methods. The presented MPPT algorithm is advantageous in being sensorless, converging quickly and requiring no prior knowledge of system parameters. The improved performance of the algorithm in terms of tracking efficiency has been validated through simulation using MATLAB/Simulink. The simulation results confirm that the proposed algorithm has a better performance in terms of tracking efficiency and energy extracted. The tracking efficiency of the proposed MPPT algorithm could reach up to 99.4% with 1.9% more harvested electrical energy than the conventional MPPT algorithms. In addition, experiments have been carried out to demonstrate the validity of the proposed MPPT algorithm. The experimental results compare well with system simulation results, and the proposed algorithm performs well, as expected.

The rest of the paper starts with a review on the related work on MPPT algorithms for WECSs in section II. Subsequently, an overview of the studied system is presented in section III, followed by descriptions of the OPP, PSO, and the proposed hybrid PSO-ORB MPPT algorithms in section IV. Section V then discusses the simulation results and a compares the proposed hybrid algorithm with conventional MPPT algorithms. The experimental setup and the validation results are presented and discussed in section VI. Finally, section VII summarizes and conclude the paper.

II. RELATED WORK

The MPPT algorithm should have the advantages of being sensorless, independent, simple, and fast in tracking. One existing MPPT algorithm is the ORB MPPT algorithm. The ORB MPPT algorithm aims to maximize power harvesting without wind speed measurements [13]. In this type of MPPT algorithm, the tracking of the maximum power is guided by a control reference. The control reference is acquired from a lookup table or from a pre-determined relationship. To build the lookup table, it is possible to use either the maximum output power and the corresponding wind turbine speed [14], [15] or maximum output power and the dc-link voltage [16]. To track the maximum power with a direct pre-determined relationship, one option is to use the mechanical torque as a function of the rotational speed equation. This method is called Optimum Torque Control (OTC) [17]. Another option is to use the equation of the optimal reference dc current as a function of the dc voltage $I_{dc\_opt} = f(V_{dc})$. Based on this relationship, a new MPPT algorithm has been proposed in [18], called a One-Power-Point (OPP) MPPT algorithm.

To track the maximum power points (MPPs) using the OPP MPPT algorithm, one maximum power status point for any specific wind speed in the working range should first be obtained [13], [19]. If this maximum point is obtained, the pairs of dc voltage and current (V_{dc}, I_{dc}) at that point are measured. The optimum coefficient is then calculated, based on the measured voltage and current. Once the optimum coefficient is known, the MPP tracking is achieved simply by calculation.

The optimum coefficient at a particular wind speed can be obtained either by offline or online MPPT algorithms. An example of the offline MPPT algorithm is the OTC used in [18]. However, offline algorithms usually have the disadvantage of optimizing the mechanical energy harvested by the wind turbine, which is not equivalent to optimizing the electrical energy delivered to the load. It has been established in studies [20]–[23] that the locations of the maximum points of mechanical and electrical power do not coincide. In addition, offline methods require knowledge of the system parameters, which are either unknown or inaccurate. Moreover, determining the optimum coefficient based on the offline algorithms implies that this coefficient remains constant throughout the wind generation system's operational lifetime. This is a wrong assumption in the real environment, where this coefficient changes with time due to a possible drift in the system parameters and due to the non-constant efficiencies of generator–converter subsystems [19], [20].

The optimum coefficient can be also obtained using the online MPPT algorithms. For example, the conventional Perturb and Observe (P&O) method has been successfully used in [24]. The conventional P&O method, which is also known as the Hill-Climbing Searching (HCS) method, is a mathematical optimization technique used to search for the local peak points of a given function. It is widely used in WECS to obtain the optimal operating point that maximizes the extracted electrical energy. This method is based on perturbing a control variable in small steps and observing the resulting changes in the target function [8]. When the target function's values do not change, the perturbations are stopped. Because the P&O MPPT algorithm is system independent and its tracking is not affected by the turbine or generator parameter shifts, it is an effective alternative for the offline MPPT algorithms [13]. However, the main drawback of the conventional P&O MPPT algorithm is the difficulty in choosing an appropriate perturbation (step size). Larger perturbation means a faster response but more oscillations around the peak point, and hence, less efficiency; smaller step size improves the efficiency but slows down the convergence speed [20], [25], [26].

The response speed as well as the tracking efficiency can be improved significantly using the PSO MPPT algorithm, due to its automated step size adaptability [11]. According to [27], [28], PSO has a simple structure, is computationally less expensive, and is easy to incorporate for online applications. As an MPPT algorithm, the PSO technique has recently been employed by a few researchers for photovoltaic (PV) systems [27], [29]–[35]. These studies employed conventional PSO and/or improved versions of PSO for enhanced tracking efficiency. Most of the studies confirmed the superiority of the PSO-based method over the conventional P&O method. For WECSs, the PSO-based MPPT algorithm has been compared with the conventional P&O MPPT algorithm in [36], and the performance of the PSO-based MPPT algorithm has been proven to be better than that of the conventional P&O MPPT algorithm.

In this paper, a solution for obtaining an accurate optimum coefficient without the need for system parameters or mechanical sensors is proposed. The solution is based on combining the PSO and ORB MPPT algorithms. The PSO MPPT algorithm is used to search for the optimum coefficient. Once the optimum coefficient is obtained, the proposed algorithm switches to the ORB MPPT mode of operation.

III. SYSTEM OVERVIEW

Figure 1 is the schematic diagram of the WECS incorporating an MPPT algorithm and a controller. The system consists of a permanent magnet synchronous generator (PMSG) driven by a wind turbine which is interfaced to the dc-bus through a rectification stage and a boost converter. In this paper, for the purpose of reducing time significantly, the average models of the rectifier-PMSG and the boost dc-dc converter were used for simulation. The average models and the turbine characteristics are presented and discussed in [24].

Referring to Figure 1, it can be seen that the optimal dc current generated by the proposed MPPT algorithm is used as a reference current (I_{dc-opt}) and it is compared to the actual input current (I_{dc}) of the boost converter. The output difference is passed to a controller to generate the corresponding duty-cycle, d.

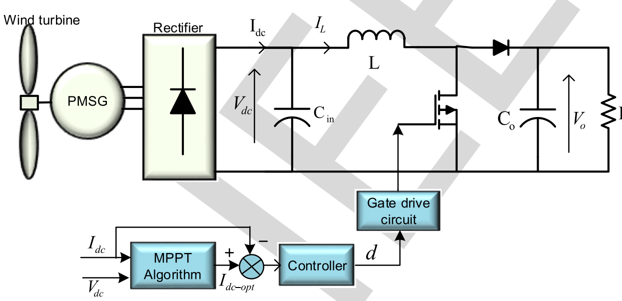

FIGURE 1. WECS configuration.

IV. THE MPPT ALGORITHMS

A. THE OPP MPPT ALGORITHM

To implement the OPP MPPT algorithm, only one initial maximum power point condition for a local wind speed needs to be obtained. At this point, the dc voltage and current are measured, then the optimum coefficient (K_{opt}) is derived. The optimum relationship is given in (1) and (2) [18], [24].

$$I_{dc-opt} = K_{opt} V_{dc}^2 \tag{1}$$

$$K_{opt} = \frac{I_{dc-peak}}{V_{dc-peak}^2} \tag{2}$$

where $I_{dc-peak}$ and $V_{dc-peak}$ are the dc current and dc voltage corresponding to the MPP at a specific wind speed.

B. THE PSO-BASED MPPT ALGORITHM

PSO is a computational method that optimizes a problem by iteratively improving a candidate solution with regard to a given measure of quality [33], [34], [37], [38]. This starts with a group of random potential solutions, which are called particles. These particles are moved around in a multi-dimensional search space in a search for the optimum solution. The next position depends on each particle's best known position, as well as the best known position of the other particles taken as a whole (the swarm). The particle position and velocity are updated iteratively based on the following two equations [30], [39], [40].

$$x_i^{k+1} = x_i^k + v_i^{k+1} \tag{3}$$

$$v_i^{k+1} = w\, v_i^k + c_1 r_1 \left\{ P_{besti} - x_i^k \right\} + c_2 r_2 \left\{ G_{besti} - x_i^k \right\} \tag{4}$$

where w is the inertia weight, c_1 and c_2 are the acceleration coefficients, r_1 and r_2 are two random values between (0, 1), P_{besti} is the personal best position of particle i, and G_{best} is the best position of the particle swarm.

In order to implement the PSO method for MPPT in this study, the position (x) variables in (3) and (4) are taken as the current references ($I_{dc,ref}$), whilst the velocity (v) variables are the correction terms for the current references (Φ). The aim of the PSO-based MPPT algorithm is to maximize the converter input power. As depicted in Figure 2, the particle position and the velocity are updated iteratively based on the following two equations:

$$\Phi_i^{k+1} = w\, \Phi_i^k + c_1 r_1 \left\{ I_{Pbest}^k - I_{dc,i}^k \right\} + c_2 r_2 \left\{ I_{gbest}^k - I_{dc,i}^k \right\} \tag{5}$$

$$I_{dc,i}^{k+1} = \Phi_i^{k+1} + I_{dc,i}^k \tag{6}$$

where $I_{dc,i}^k$ is the input current reference, $I_{dc,i}^{k+1}$ is the modified input current reference, and I_{Pbest}^k is the personal best input current; I_{gbest}^k is global best input current, Φ_i^k is the current perturbation, and Φ_i^{k+1} is the modified perturbation.

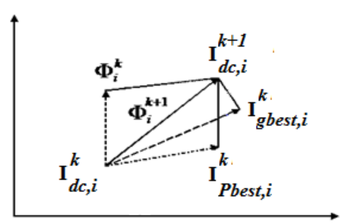

FIGURE 2. Concept of modification of a searching point by PSO.

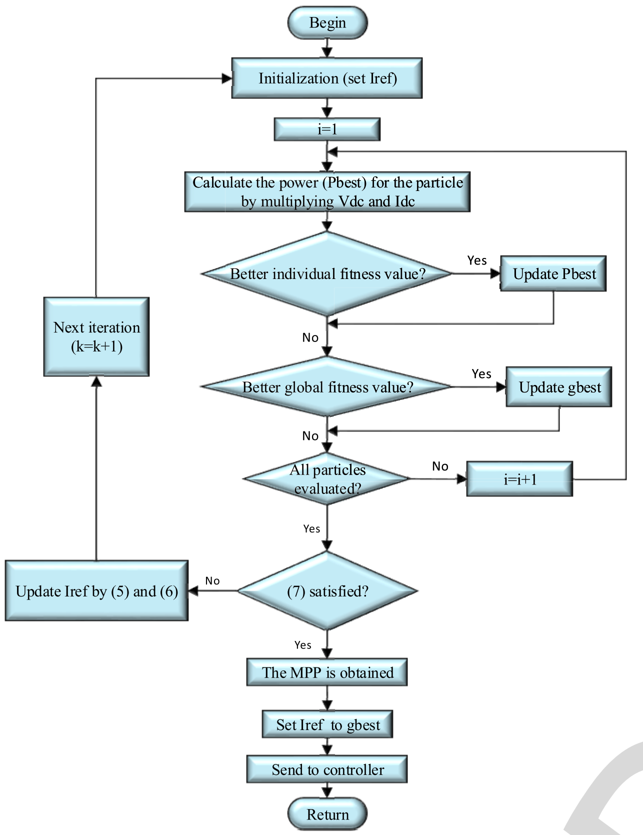

FIGURE 3. The flow chart for the PSO-based MPPT.

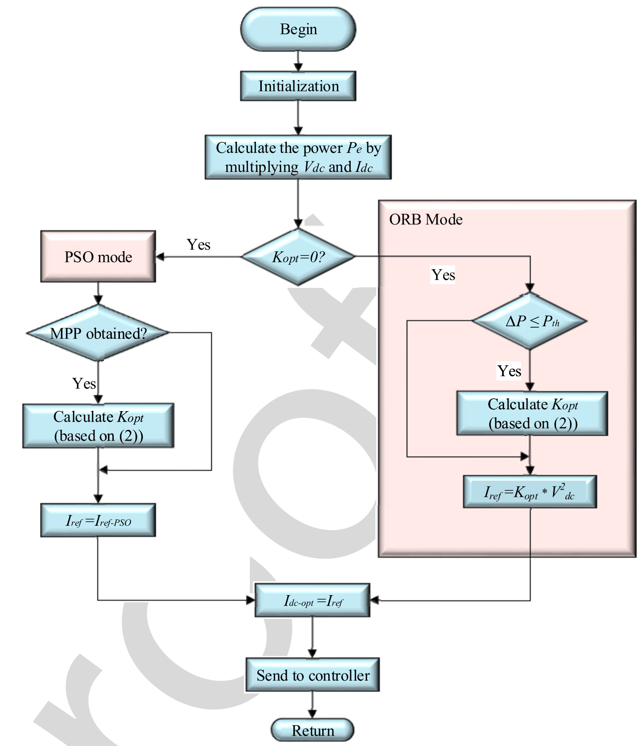

FIGURE 4. The flow chart for the proposed PSO-ORB MPPT.

The flow chart for the PSO-based MPPT algorithm applied for the WECS system is shown in Figure 3 as was described in [36]. Based on the flow chart, to start the optimization process, the PSO-based MPPT algorithm sends initial values of the dc current reference to the converter controller and senses the produced power. Then, based on (5) and (6), the algorithm updates the dc current reference and sends the new currents to the converter controller. The process of generating new references and calculating the corresponding power continues until the convergence criterion defined in (7) is satisfied. This is to ensure that all the particles converge to the MPP.

$$\left|P_{gbest} - P_{new,i}\right| < P_{th}; \quad i = 1 \ldots n \tag{7}$$

where P_{gbest} is the global best fitness and P_{th} is a threshold value.

C. THE PROPOSED HYBRID PSO-ORB MPPT ALGORITHM

One simple and effective solution to overcome the drawbacks in obtaining the optimum coefficient in the conventional ORB MPPT algorithm is to incorporate a self-tuning capability using the conventional PSO method.

The hybrid PSO-ORB MPPT algorithm can accurately obtain the optimum electrical power versus dc current curve and track the maximum power peaks at different wind speeds, without the turbine characteristics and the rotor and wind speed measurements. Figure 4 illustrates the flow chart of the proposed hybrid algorithm. As shown in the figure, the flow of the operation consists of two modes, namely the PSO mode and the ORB mode. In the first mode, the PSO-based algorithm is employed to search for the optimum relationship between the dc power and dc current. Once the convergence criterion in (7) is satisfied, the optimum coefficient (K_{opt}) is calculated using (2) based on the measured dc voltage and dc current. The second mode only will be activated once the value of K_{opt} is determined.

One of the differences between the conventional ORB MPPT algorithm and the proposed MPPT algorithm is that K_{opt} is updated continuously once any maximum power point is detected. This, in turn, improves the tracking efficiency by solving the non-uniqueness problem of the optimum curve.

Using the PSO MPPT algorithm to extract the value of K_{opt} avoids the need to know the system parameters. It also improves the MPPT efficiency, because of its reliance on optimizing electrical power rather than mechanical power.

V. SIMULATION RESULTS AND DISCUSSION

In this section, MATLAB/Simulink software is used to verify the performance of the proposed MPPT algorithm. The parameters of the wind turbine, PMSG, and the boost converter are listed in Table 1.

A. THE OPP MPPT ALGORITHM

To implement the OPP MPPT algorithm, the calculation of the unknown coefficient (K_{opt}) in (1) should be obtained first. Obtaining K_{opt} is based on simulating the conventional

TABLE 1. Parameters of the simulated system.

Wind Turbine			PMSG			Boost Converter		
ρ:	1.08	kg/m^3	R_w:	3.6	Ω	L	1	mH
R:	2.3	m	K_w:	2.25	V.s/rad	C_{in}	470	μF
J:	0.4	kg.m^2				C_o	470	μF

OTC MPPT algorithm and then using the measured dc voltage and current at a one MPP for the calculation.

The simulation results of the simulated OTC MPPT algorithm for the range of wind speeds between 6 m/s and 9 m/s are tabulated in Table 2. According to reference [18], it is recommended that K_{opt} should be calculated using the mean wind speed of the simulated wind profile in order to reduce the non-linearity relation effect in (1). The mean wind speed is 7.5 m/s and the corresponding optimum voltage and current are 48 V and 3.07 A, respectively. The calculated K_{opt} at 7.5 m/s wind speed is 1.33247×10^{-3}. From this table, it can be seen that K_{opt} is not a constant value, but varies with respect to wind speeds. In other words, the calculated K_{opt} is non-unique– it is specific for each wind speed.

TABLE 2. The calculated K_{opt} based on the optimum voltage and current in OTC MPPT algorithm.

Wind speed (m/s)	Optimum dc voltage (V)	Optimum dc current (A)	Optimal parameter K_{opt}
6.0	40.23	1.96	1.21103×10-3
6.5	43.00	2.30	1.24392×10-3
7.0	45.56	2.67	1.2863×10-3
7.5	48.00	3.07	1.33247×10-3
8.0	50.50	3.50	1.37241×10-3
9.0	55.00	4.42	1.46116×10-3

Based on the selected K_{opt} at 7.5 m/s wind speed, the I_{dc} versus V_{dc}^2 curves are plotted in Figure 5. The optimal I_{dc} line in the figure is the optimal relationship between I_{dc} and V_{dc}^2 for the given design (parameters in Table 1). The five points

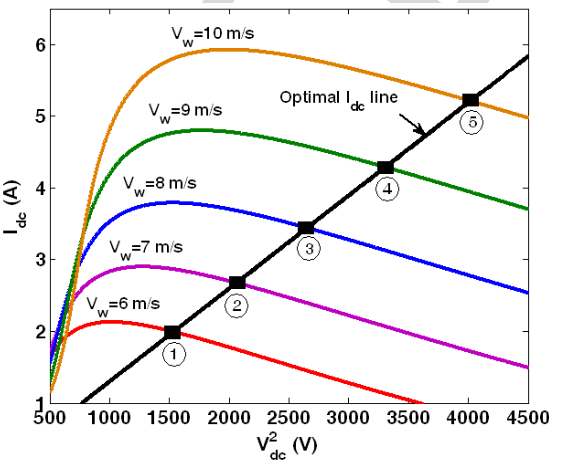

FIGURE 5. The characteristic curves of I_{dc} as a function of V_{dc}^2 at different wind speeds.

shown in the figure are the optimum voltage and current at the corresponding wind speeds. If the WECS operates continually based on this optimal I_{dc} line, it would ensure that the extracted power from the wind is close to the optimum.

Figure 6 shows the mechanical power as a function of dc current. The figure shows that the MPPs can be tracked by operating the WECS system constantly on the optimal current curve (as represented by (1)). Another significant observation that should be noted in the figure is the permitted operating range of the current. Each wind speed has a maximum current limit point: operating beyond this point would make the system decelerate drastically, and thus lead to system shutdown [41]. In Figure 6, the area above the maximum limit current curve (represented by region A) is the permitted operating region, while the area under the curve (region B) is the area where the WECS will stop generation. Therefore, the current command for a specific wind speed should not exceed the maximum limit current curve, in order to prevent system shutdown.

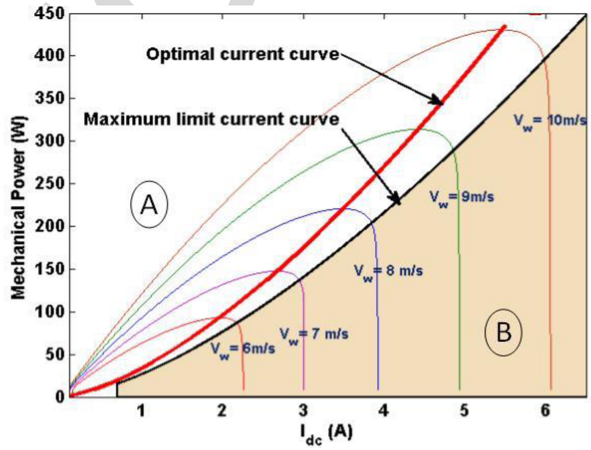

FIGURE 6. Characteristics of turbine power as a function of the dc-side current (I_{dc}) for a series of wind speeds.

It has been mentioned in the introduction that calculation of K_{opt} based on the offline algorithms, such as an OTC algorithm, reduces the extracted energy. This is because an OTC algorithm actually optimizes the mechanical power (P_m), which has maximum peak points at different locations from those for the electrical power (P_e). To illustrate this, the loci of maximum mechanical power($P_{m\ \max}$)and maximum electrical power ($P_{e\ \max}$) are represented graphically, below. The mechanical and electrical power at 8 m/s wind speed are plotted as a function of the dc current, in Figure 7. It can be seen that, although the peak point of mechanical power is at 3.5 A dc current, the maximum electrical power is at 3.2 A dc current.

Generally, equation (1) together with Figure 6 implies that if the K_{opt} at any specific wind speed within the simulated profile is known, it is possible to obtain the optimum curve to implement the ORB MPPT algorithm. Although this algorithm is preferable because of its ease of implementation and

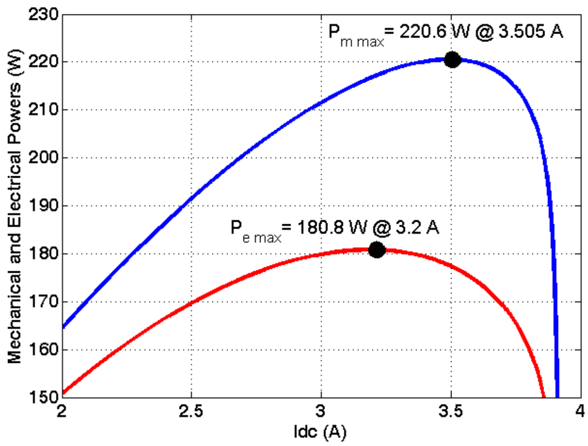

FIGURE 7. **The mechanical power (P_m) and the electrical power (P_e) curves at a wind speed of 8 m/s.**

fast tracking ability, in order to calculate K_{opt} one peak point of the mechanical power versus dc current curves and its corresponding voltage and current are required. One of the drawbacks in an ORB MPPT algorithm is the difficulty of obtaining this value. Another drawback is the non-uniqueness of the obtained curve. In addition, the ORB MPPT algorithm is customized for a particular wind turbine, as it strongly depends on the wind turbine parameters. Furthermore, this algorithm assumes a certain value of air density in all calculations; however, air density in a real environment is subject to atmospheric changes.

B. THE PSO-BASED MPPT ALGORITHM

In order to evaluate the performance of the PSO-based MPPT algorithm for WECS, two different simulation studies were carried out. In the first case the wind speed is steeply changed from 6 m/s to 8 m/s, whereas in the second case the wind speed is changed from 8 m/s to 7.5 m/s.

For the first case it is assumed that the wind speed is stable at 6 m/s and the dc current is regulated at 1.84 A. A swarm of three particles with an initial vector position of [2.04 A, 2.24 A and 2.44 A] has been arbitrarily chosen for the first iteration. Because the converter can only respond to one command at a time, the particles are initialized and evaluated in a successive manner. It is important for the system to reach the steady state before taking the next sample. The PSO parameters employed in this work are tabulated in Table 3.

TABLE 3. **The values of the PSO parameters used in the simulation.**

w	c_1	c_2	r_1	r_2	P_{th}
0.15	0.5	1.6	1	1	0.05

The tracking process of the PSO-based MPPT algorithm is displayed in Figure 8 and Figure 9. Figure 8 shows the particles' movement during the tracking process for the first case of simulation, where the PSO-based MPPT algorithm

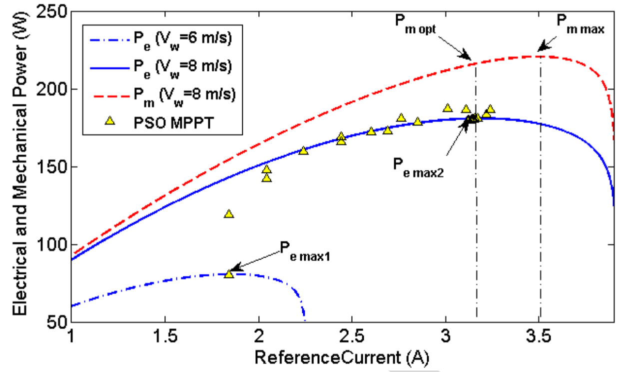

FIGURE 8. **The operating points of the PSO-based MPPT algorithm tracking process under the first case (6 m/s to 8 m/s wind speed).**

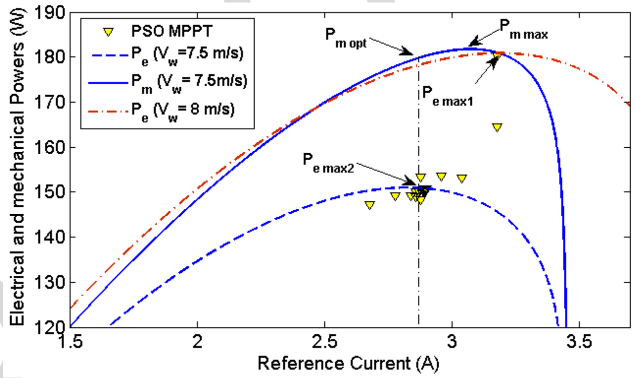

FIGURE 9. **The operating points of the PSO-based MPPT algorithm tracking process under the second case (8 m/s to 7.5 m/s wind speed).**

works by moving a sequence of improved particles towards the optimum solution. It can be seen from the figure that the PSO-based MPPT algorithm has converged to the correct MPP. Unlike the conventional ORB algorithm simulated in the previous section, the PSO-based MPPT algorithm optimizes the electrical power but not the mechanical power. The stopping criterion in (7) is satisfied at 3.16 A dc current, which corresponds to 180.3 W.

The second set of the simulation is displayed in Figure 9. It can be seen from the figure that the algorithm has successfully tracked the correct maximum point of the electrical power. The maximum peak power that is computed by the algorithm in this case is 150.5 W at a dc current of 2.88 A.

The detailed simulation results for the two cases will be described in the next section. However, it can be concluded from the explanations above that the PSO-based MPPT algorithm is capable of tracking the true MPP. As with all other P&O algorithms, the problem with this algorithm is that the computational time required for convergence may be long, if the range of the search space is large. In addition, the interval of time required between the successive samples affects the tracking speed, which may lead to the loss of tracking when the wind speed changes rapidly. Furthermore, in order for the WECS to avoid working beyond the conditions defined by the maximum limit current curve, the PSO-based MPPT algorithms must include that curve.

C. THE PROPOSED HYBRID PSO-ORB MPPT ALGORITHM

Assessment of the proposed MPPT algorithm is carried out by simulating two different wind speed profiles. The simulated wind profiles are based on references [18] and [41]. The wind profiles take into account the step change as well as the linear change of wind speed with different slopes. The initial interval in both cases ($t < 50$ s) is similar to that simulated in the previous section. In the first wind profile simulation (Case 1), the WECS is considered stable at the maximum peak on the wind speed curve at 6 m/s. After twenty seconds ($t = 20$ s), the wind speed is suddenly increased to 8 m/s. Similarly, in the second wind profile simulation (Case 2), the WECS is considered initially stable at a wind speed equal to 8 m/s, which then steeply drops to 7.5 m/s after twenty seconds. The simulated wind profiles have been initialized with the above-mentioned two cases in order to test the tracking capability of the PSO-based MPPT algorithm under either positive or negative wind speed changes. The rest of the intervals in both wind profiles simulate different slopes and wind speed values.

The wind profiles are depicted in Figure 10 (a) and Figure 11 (a), respectively. As shown in Figure 10 (b) and Figure 11(b), the MPPT algorithm starts in the conventional PSO mode (at $t = 20$ s) and the dc current is used as a perturbation (control) variable.

In Case 1, the algorithm transmits three dc current references to the controller, with a step-size difference of 0.2 A. Based on the three measured powers at those reference currents and according to equations (5) and (6), the PSO algorithm modifies the step sizes and then sends the new modified reference currents to the controller. Again, the electrical power corresponding to each reference current sent is measured, and a new modification for the current reference is carried out. Exploration of the search space continues until the convergence criterion (7) is satisfied. It can be observed that it takes 5 iterations (total time of 12 s) for the PSO mode to detect the MPP at 8 m/s and to calculate the parameter K_{opt} based on the corresponding measured voltage and current. The measured dc voltage and current are 57.5 V and 3.16 A, respectively. At $t = 31.2$ s the value of K_{opt} is obtained and the algorithm switches to the second mode of operation (ORB mode). The optimal reference current is then calculated directly, based on (1).

In Case 2, a similar scenario to the search in Case 1 is found. It can be seen from Figure 11(b) that three current reference values [3.18 A, 2.78 A, 2.68 A] are sent to the controller in the first iteration of the PSO mode. It is worth mentioning that a step size of 0.4 A (the difference between 3.18 A and 2.78 A) was decided upon to avoid working beyond the maximum current curve corresponding to a wind speed of 7.5 m/s. This takes the algorithm approximately 19 s to track the new maximum peak at 7.5 m/s and to calculate the K_{opt} successfully.

The step size of the PSO-based MPPT algorithm is adaptive. From the figures, it can be seen that the maximum step size reaches 0.56 A and 0.4 A during the tracking process intervals in Case 1 and Case 2, respectively. Nonetheless, it approaches zero when it converges to the optimal power points.

Referring to Figure 10 (c) and Figure 11 (c), it can be clearly seen that in contrast to the conventional simulated MPPT algorithms, the power coefficient for the proposed hybrid algorithm is not constant. Although operating the WECS at the maximum power coefficient means the harvested mechanical power is maximized, nevertheless, as previously discussed, the peaks of the electrical power curves do not coincide with the peaks of the mechanical power curves. Consequently, for efficient tracking of the maximum electrical power, the WECS should not operate at the maximum power coefficient. In addition, it can be observed from the figures that despite a very short time and large variations in the power coefficient during the transient process, it is regulated to return to its optimal values quite fast– even for large step changes in wind speed.

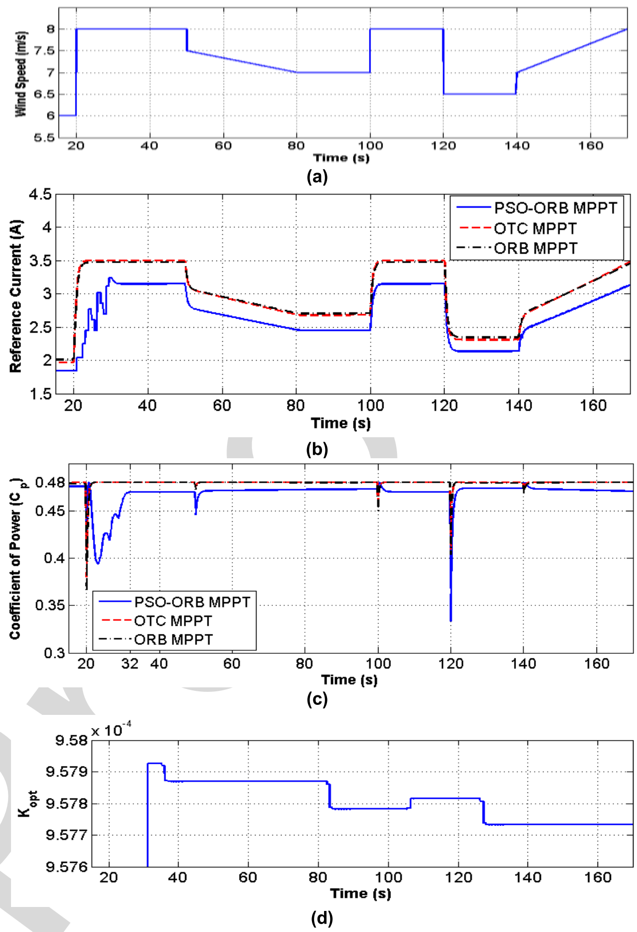

FIGURE 10. The proposed hybrid PSO-ORB MPPT simulation: Case 1 (a) variation in the wind speed (b) the calculated reference current from the MPPT ($I_{ref-opt}$) (c) the corresponding coefficient of power (C_p) (d) the corresponding K_{opt}.

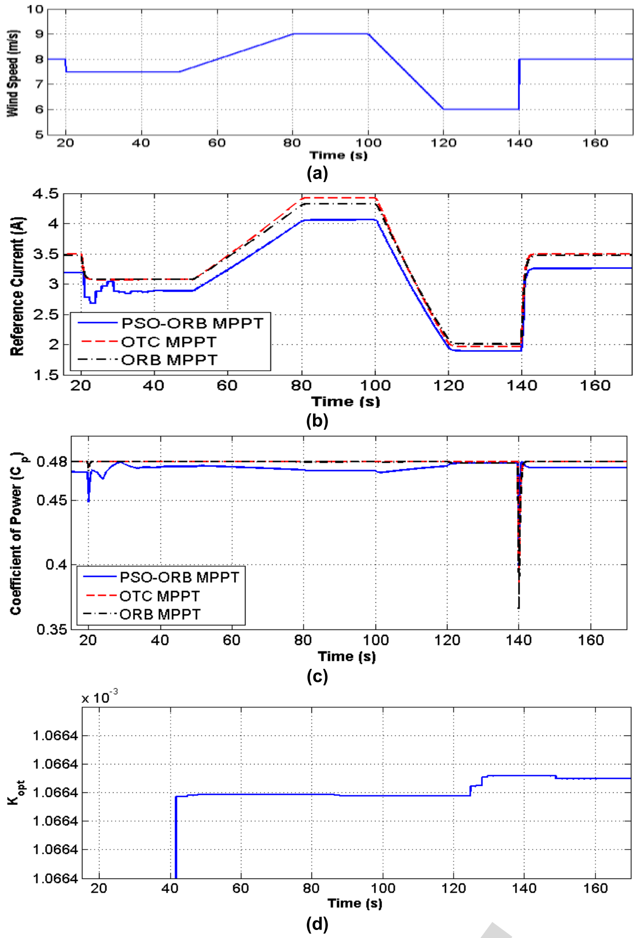

FIGURE 11. The proposed hybrid PSO-ORB MPPT simulation: Case 2 (a) variation in the wind speed (b) the calculated reference current from the MPPT ($I_{ref-opt}$) (c) the corresponding coefficient of power (C_p) (d) the corresponding K_{opt}.

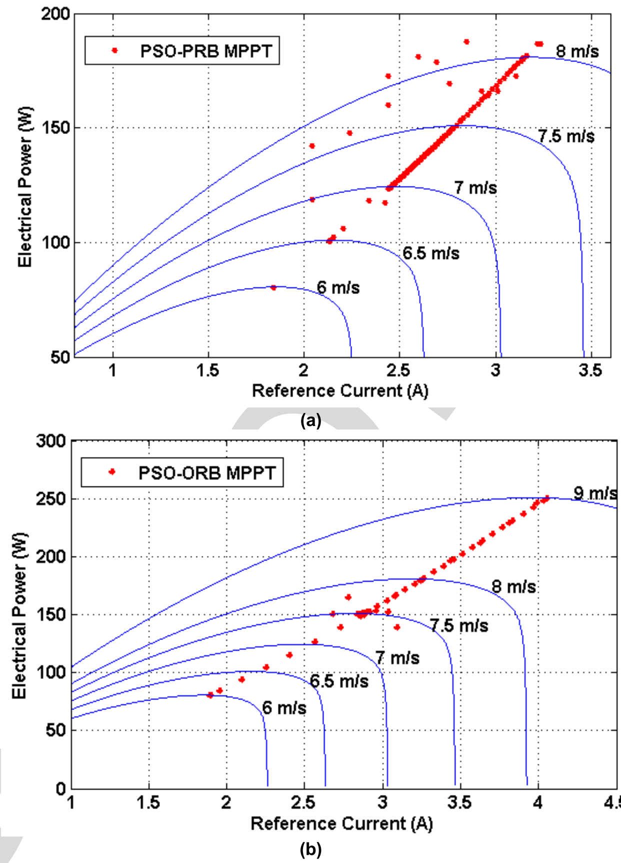

FIGURE 12. Tracking curves of the (a) Case 1 (b) Case 2.

It was mentioned in the introduction that one advantage of the proposed algorithm is the adaptability of the optimum curves. This claim is confirmed, as depicted by the K_{opt} curves in Figure 10 (d) and Figure 11 (d).

The loci of the tracking operating points for Case 1 and Case 2 are shown in Figure 12 (a) and (b). It can be seen from the figures that the peak power points at different wind speeds have been tracked correctly and efficiently.

D. SIMULATION COMPARISON OF OTC, ORB AND PSO-ORB MPPT ALGORITHMS

For performance comparison, the existing algorithms, namely the conventional OTC algorithm and the conventional ORB algorithm were also simulated for MPP tracking under identical conditions.

The electrical and mechanical power obtained for the two simulated wind profiles employing the OTC, ORB, and PSO-ORB MPPT algorithms are plotted in Figure 13 and Figure 14. The simulation results of the electrical power are also summarized in Table 4. In the table, the tracking efficiency is calculated by taking the ratio between the maximum effective power obtained from the theoretical curve and the corresponding MPP detected at a given wind speed. Figure 15 shows the tracking efficiency for the tested wind speeds. From the figure and table, it can be observed that when the wind velocity increases, the efficiency of the OTC algorithm decreases, while the efficiencies of the ORB and PSO-ORB improve. At all wind speeds, the proposed hybrid PSO-ORB MPPT algorithm has the highest tracking efficiency, where the generated electrical power almost fits the maximum effective output curve. It is noted that the efficiency of the PSO-ORB MPPT algorithm varies between 99.1% and 99.7%, with an average efficiency of 99.4%.

In order to evaluate the effectiveness of the PSO-ORB algorithm, the electrical energy captured by the WECS for the simulated wind profiles has been computed and compared with that obtained when the latter is controlled by the OTC, as well as when it is controlled by the ORB MPPT algorithm. As can be seen from Table 5, the proposed MPPT algorithm has a higher energy output. The overall power efficiency using the hybrid PSO-ORB MPPT algorithm is approximately 1.9% higher than when using the conventional OTC and ORB MPPT algorithms. The overall power efficiency is calculated by taking the ratio of the electrical energy obtained from the theoretical curve to that produced by the corresponding MPPT algorithm for the simulated wind profiles.

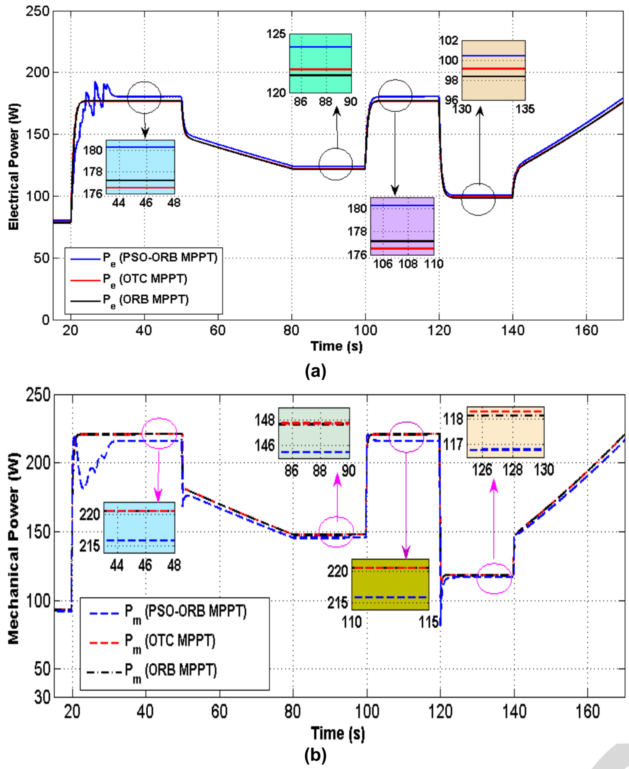

FIGURE 13. Performance comparison: Case 1 (a) electrical power (b) mechanical power.

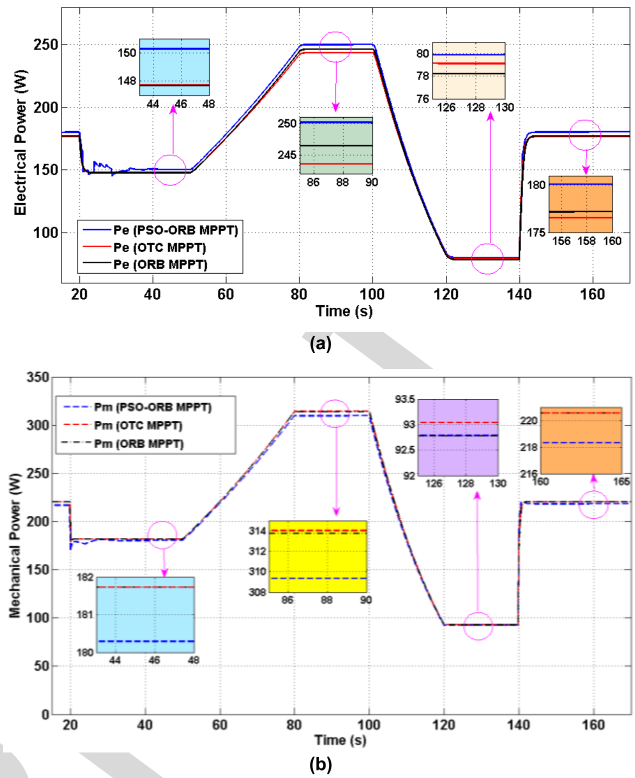

FIGURE 14. Performance comparison: Case 2 (a) electrical power (b) mechanical power.

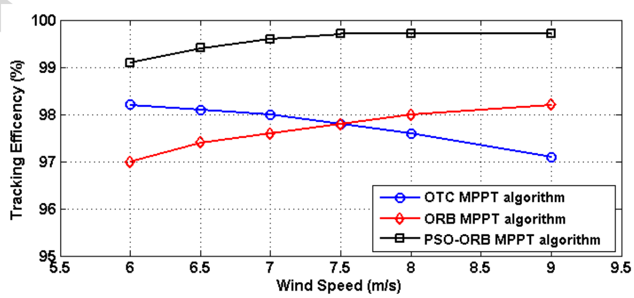

FIGURE 15. Tracking efficiency at the simulated wind speeds.

In the proposed hybrid MPPT algorithm no off-line experiments are required and the accurate optimum relationship can be obtained in variable wind conditions. In addition, online optimization of the electrical power improves the energy output from the WECS. Another advantage of using the proposed hybrid algorithm is that the search space for the PSO is reduced, and hence, the time that is required for convergence can be greatly decreased. Moreover, the possibility of entering the region beyond the maximum current limit curve is reduced, due to the very fast detection and response of the ORB MPPT algorithm. This ensures continuous power generation from the WECS.

VI. EXPERIMENTAL RESULTS AND DISCUSSION

The hardware design of the overall system is represented by the block diagram shown in Figure 16. In order to test the proposed MPPT algorithm, a flexible WECS is required. For that reason, a simplified wind generator emulator was developed. The main objective of the emulator is to obtain the same voltage variation as from a real wind generator.

The wind generator emulator is a controllable dc voltage source, which is controlled to provide the same voltage characteristic as the wind energy generation system. The wind generator emulator is implemented with a boost dc-dc converter and a constant dc voltage source (as shown in Figure 16). By controlling the output voltage of the boost converter (V_{dc}), the wind generator voltage characteristics can be emulated. The control action is achieved using the duty ratio of the switch (Q_1) as a control variable.

For comparison, the same test conditions and environment have been set for both the MATLAB/Simulink simulation and the experiments. The objective of the experiments is to prove that the performance is in agreement with the simulation results. Because of the limitations in the ratings of some equipment, the exact test conditions previously simulated in section 4 are not replicated. Rather, new test conditions are simulated and compared with the experimental results.

To test the functionality of the proposed hybrid PSO-ORB MPPT algorithm, simulated changes in wind speed (V_w) are applied to the WECS, as shown Figure 18 (a).

TABLE 4. Summary of performance comparison of OTC, ORB and PSO-ORB MPPT algorithms in terms of tracking efficiency.

Wind speed (m/s)	Tracking algorithm	Simulated P_e (W)	Maximum power from power-current curve (W) P_e	Tracking efficiency (%) η_e
6.0	OTC	79.11	80.59	98.2
	ORB	78.20		97.0
	PSO-ORB	79.86		99.1
6.5	OTC	99.11	101.00	98.1
	ORB	98.33		97.4
	PSO-ORB	100.40		99.4
7.0	OTC	121.95	124.40	98.0
	ORB	121.40		97.6
	PSO-ORB	123.90		99.6
7.5	OTC	147.72	151.00	97.8
	ORB	147.70		97.8
	PSO-ORB	150.50		99.7
8.0	OTC	176.53	180.80	97.6
	ORB	177.20		98.0
	PSO-ORB	180.30		99.7
9.0	OTC	243.52	250.80	97.1
	ORB	246.40		98.2
	PSO-ORB	250.10		99.7

TABLE 5. Electrical Energy harvested by OTC, ORB and PSO-ORB MPPT algorithms.

Simulated profile	Tracking algorithm	Electrical energy (W·s)	Average P_e	Overall power efficiency (%)
Case 1	Theoretical	25922.70	172.8	--
	OTC	25275.70	168.5	97.5
	ORB	25396.50	169.3	97.8
	PSO-ORB	25831.80	172.2	99.6
Case 2	Theoretical	22257.00	148.4	--
	OTC	21769.95	145.1	97.8
	ORB	21770.10	145.1	97.8
	PSO-ORB	22180.00	147.9	99.7

The WECS operates at 5 m/s until a sudden rise in wind speed to 5.5 m/s occurs at t = 30 s. After that, variations between 5.5 m/s and 5 m/s, with different rates of change, occur for the rest of the interval time. The values of 5 m/s and 5.5 m/s have been selected so that the change in the produced voltages and currents are within the rating of the experimental prototype.

The dc voltage (V_{dc}) and inductor current (i_L) obtained from the simulation are shown in Figure 18 (b), while the dc voltage and inductor current obtained from the experiment are depicted in Figure 18 (c). As can be seen from the figure, although a sudden rise in the wind speed occurs at t = 30 s, the proposed hybrid PSO-ORB MPPT algorithm takes approximately 4 s to find the optimal inductor current

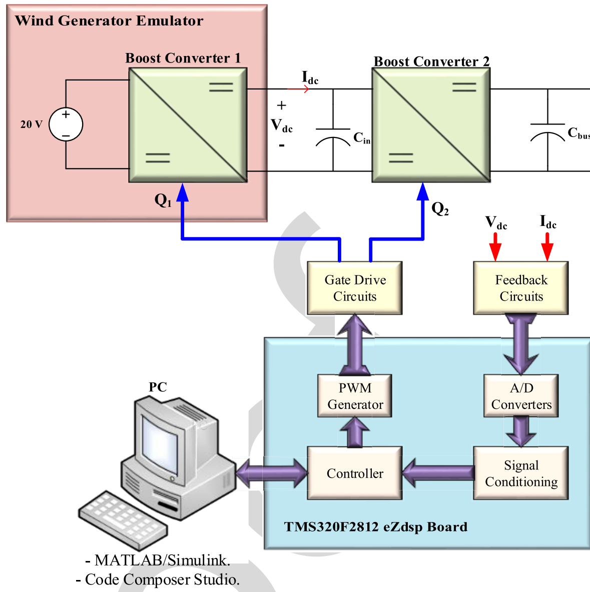

FIGURE 16. The system implementation block diagram.

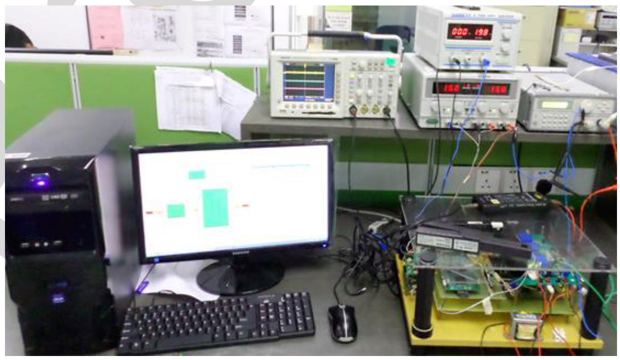

FIGURE 17. A photograph of the laboratory experimental set-up.

corresponding to the maximum power of 5.5 m/s. During these four seconds, the proposed algorithm works in the PSO mode. After t = 34 s, each change in wind speed is immediately followed by a change in the inductor current. This is because the optimum coefficient of the ORB MPPT algorithm was already calculated, and hence, the proposed MPPT algorithm is working under ORB mode during this interval of time. This demonstrates that the proposed control algorithm tracks the MPPs rapidly.

It can be noticed from the figures that the change in wind speed is also reflected in a change in the dc voltage. The dc voltage is actually the emulation of the wind generator voltage that is generated from the wind generator model represented in MATLAB/Simulink. This is a proof that wind generator emulator is capable of achieving the desired objective.

A slight difference between the simulation and the experimental results is observed as a result of parasitic effects of the converter elements, which are not taken into account in the simulated average models in MATLAB/Simulink.

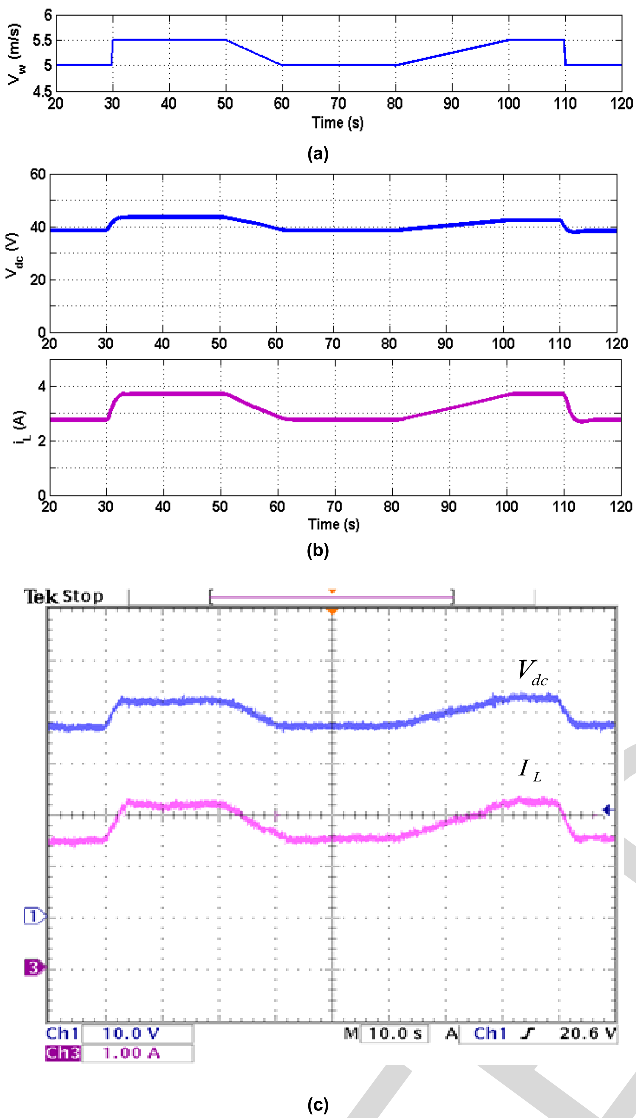

FIGURE 18. **The proposed MPPT algorithm test (a) simulated wind speed profile (b) simulation results (c) experimental results.**

VII. CONCLUSION

In this paper a new MPPT algorithm for WECS based on a combination of the conventional PSO and ORB MPPT algorithms has been presented. The proposed hybrid method has two operational modes, namely PSO mode and ORB mode. During the PSO mode, the PSO MPPT algorithm is used for searching for one peak point, at any wind speed, and then the measured voltage and current at that point are used to calculate the unknown coefficient of the ORB MPPT algorithm. Once the unknown coefficient is calculated, it can be used for calculating the optimal reference current for MPP tracking.

The performance of the proposed MPPT algorithm has been investigated by simulating the proposed algorithm using MATLAB/Simulink and comparing the simulation results with those obtained with conventional OTC and ORB MPPT algorithms. The proposed MPPT algorithm offers several advantages: (1) no mechanical sensors are needed, (2) no prior knowledge of system parameters is needed, (3) the optimization is performed for the electrical power rather than the mechanical power, which improves the WECS' efficiency. The simulation results obtained have confirmed that the tracking performance is improved and the energy harvested from the wind is increased. Based on the simulated wind profiles, the tracking efficiency of the proposed algorithm could reach up to 99.7%. In addition to that, the harvested electrical energy is 1.9% higher than that using the conventional OTC and ORB MPPT algorithms. The proposed MPPT algorithm was successfully implemented and obtained promising results which compare well with the simulation results.

REFERENCES

[1] A. Navidi and F. A.-S. Khatami, "Energy management and planning in smart cities," *CIRED—Open Access Proc. J.*, vol. 2017, no. 1, pp. 2723–2725, 2017. AQ:5

[2] A. Gaur, B. Scotney, G. Parr, and S. McClean, "Smart city architecture and its applications based on IoT," *Procedia Comput. Sci.*, vol. 52, pp. 1089–1094, Jan. 2015.

[3] R. Petrolo, V. Loscri, and N. Mitton, "Towards a smart city based on cloud of things," in *Proc. ACM Int. Workshop Wireless Mobile Technol. Smart Cities*, 2014, pp. 61–66.

[4] K. Kumar, S. Kumar, O. Kaiwartya, Y. Cao, J. Lloret, and N. Aslam, "Cross-layer energy optimization for IoT environments: Technical advances and opportunities," *Energies*, vol. 10, no. 12, p. 2073, 2017.

[5] Y. Cao *et al.*, "Mobile edge computing for big-data-enabled electric vehicle charging," *IEEE Commun. Mag.*, vol. 56, no. 3, pp. 150–156, Mar. 2018.

[6] Y. Cao, O. Kaiwartya, Y. Zhuang, N. Ahmad, Y. Sun, and J. Lloret, "A decentralized deadline-driven electric vehicle charging recommendation," *IEEE Syst. J.*, to be published. AQ:6

[7] M. A. Abdullah, A. H. M. Yatim, C. W. Tan, and R. Saidur, "A review of maximum power point tracking algorithms for wind energy systems," *Renew. Sustain. Energy Rev.*, vol. 16, no. 5, pp. 3220–3227, 2012, doi: 10.1016/j.rser.2012.02.016.

[8] D. Zammit, C. S. Staines, A. Micallef, M. Apap, and J. Licari, "Incremental current based MPPT for a PMSG micro wind turbine in a grid-connected DC microgrid," *Energy Procedia*, vol. 142, pp. 2284–2294, Dec. 2017.

[9] H. T. Do, T. D. Dang, H. V. A. Truong, and K. K. Ahn, "Maximum power point tracking and output power control on pressure coupling wind energy conversion system," *IEEE Trans. Ind. Electron.*, vol. 65, no. 2, pp. 1316–1324, Feb. 2018.

[10] M. H. Ali, *Wind Energy Systems: Solutions for Power Quality and Stabilization*. London, U.K.: Taylor & Francis, 2012.

[11] M. A. Abdullah, "Control of energy conversion in a hybrid wind and ultracapacitor energy system," Ph.D. dissertation, Elect. Power Eng., Universiti Teknologi Malaysia, Johor Bahru, Malaysia, 2015.

[12] J. P. Ram, N. Rajasekar, and M. Miyatake, "Design and overview of maximum power point tracking techniques in wind and solar photovoltaic systems: A review," *Renew. Sustain. Energy Rev.*, vol. 73, pp. 1138–1159, Jun. 2017.

[13] Y. Xia, K. H. Ahmed, and B. W. Williams, "Wind turbine power coefficient analysis of a new maximum power point tracking technique," *IEEE Trans. Ind. Electron.*, vol. 60, no. 3, pp. 1122–1132, Mar. 2013. AQ:7

[14] S. M. Barakati, M. Kazerani, and J. D. Aplevich, "Maximum power tracking control for a wind turbine system including a matrix converter," *IEEE Trans. Energy Convers.*, vol. 24, no. 3, pp. 705–713, Sep. 2009.

[15] K. Tan and S. Islam, "Optimum control strategies in energy conversion of PMSG wind turbine system without mechanical sensors," *IEEE Trans. Energy Convers.*, vol. 19, no. 2, pp. 392–399, Jun. 2004.

[16] Q. Wang and L. Chang, "An intelligent maximum power extraction algorithm for inverter-based variable speed wind turbine systems," *IEEE Trans. Power Electron.*, vol. 19, no. 5, pp. 1242–1249, Sep. 2004.

[17] M. Pucci and M. Cirrincione, "Neural MPPT control of wind generators with induction machines without speed sensors," *IEEE Trans. Ind. Electron.*, vol. 58, no. 1, pp. 37–47, Jan. 2011.

[18] H.-B. Zhang, J. Fletcher, N. Greeves, S. J. Finney, and B. W. Williams, "One-power-point operation for variable speed wind/tidal stream turbines with synchronous generators," *IET Renew. Power Gener.*, vol. 5, no. 1, pp. 99–108, 2011.

[19] Y. Daili, J.-P. Gaubert, and L. Rahmani, "Implementation of a new maximum power point tracking control strategy for small wind energy conversion systems without mechanical sensors," *Energy Convers. Manage.*, vol. 97, pp. 298–306, Jun. 2015.
[20] S. M. R. Kazmi, H. Goto, H.-J. Guo, and O. Ichinokura, "A novel algorithm for fast and efficient speed-sensorless maximum power point tracking in wind energy conversion systems," *IEEE Trans. Ind. Electron.*, vol. 58, no. 1, pp. 29–36, Jan. 2011.
[21] S. M. R. Kazmi, H. Goto, H.-J. Guo, and O. Ichinokura, "Review and critical analysis of the research papers published till date on maximum power point tracking in wind energy conversion system," in *Proc. IEEE Energy Convers. Congr. Expo. (ECCE)*, Sep. 2010, pp. 4075–4082.
[22] C. Vlad, I. Munteanu, A. I. Bratcu, and E. Ceangă, "Output power maximization of low-power wind energy conversion systems revisited: Possible control solutions," *Energy Convers. Manage.*, vol. 51, no. 2, pp. 305–310, 2010.
[23] H. Fathabadi, "Novel maximum electrical and mechanical power tracking controllers for wind energy conversion systems," *IEEE Trans. Emerg. Sel. Topics Power Electron.*, vol. 5, no. 4, pp. 1739–1745, Dec. 2017.
[24] M. A. Abdullah, A. H. M. Yatim, and C. W. Tan, "An online optimum-relation-based maximum power point tracking algorithm for wind energy conversion system," in *Proc. Australas. Universities Power Eng. Conf. (AUPEC)*, Sep./Oct. 2014, pp. 1–6.
[25] C. T. Pan and Y. L. Juan, "A novel sensorless MPPT controller for a high-efficiency microscale wind power generation system," *IEEE Trans. Energy Convers.*, vol. 25, no. 1, pp. 207–216, Mar. 2010.
[26] M.-K. Hong and H.-H. Lee, "Adaptive maximum power point tracking algorithm for variable speed wind power systems," presented at the Int. Conf. Life Syst. Modeling Intell. Comput., Int. Conf. Intell. Comput. Sustain. Energy Environ., Wuxi, China, 2010.
[27] K. Sundareswaran, S. Peddapati, and S. Palani, "MPPT of PV systems under partial shaded conditions through a colony of flashing fireflies," *IEEE Trans. Energy Convers.*, vol. 29, no. 2, pp. 463–472, Jun. 2014.
[28] K. Sundareswaran, S. Peddapati, and S. Palani, "Application of random search method for maximum power point tracking in partially shaded photovoltaic systems," *IET Renew. Power Gener.*, vol. 8, no. 6, pp. 670–678, 2014.
[29] K. L. Lian, J. H. Jhang, and I. S. Tian, "A maximum power point tracking method based on perturb-and-observe combined with particle swarm optimization," *IEEE J. Photovolt.*, vol. 4, no. 2, pp. 626–633, Mar. 2014.
[30] K. Ishaque and Z. Salam, "A deterministic particle swarm optimization maximum power point tracker for photovoltaic system under partial shading condition," *IEEE Trans. Ind. Electron.*, vol. 60, no. 8, pp. 3195–3206, Aug. 2013.
[31] M. K. Alam, F. Khan, and A. M. Imtiaz, "Optimization of subcell interconnection for multijunction solar cells using switching power converters," *IEEE Trans. Sustain. Energy*, vol. 4, no. 2, pp. 340–349, Apr. 2011.
[32] Y.-H. Liu, S.-C. Huang, J.-W. Huang, and W.-C. Liang, "A particle swarm optimization-based maximum power point tracking algorithm for PV systems operating under partially shaded conditions," *IEEE Trans. Energy Convers.*, vol. 27, no. 4, pp. 1027–1035, Dec. 2012.
[33] K. Ishaque, Z. Salam, M. Amjad, and S. Mekhilef, "An improved particle swarm optimization (PSO)–based MPPT for PV with reduced steady-state oscillation," *IEEE Trans. Power Electron.*, vol. 27, no. 8, pp. 3627–3638, Aug. 2012.
[34] M. Miyatake, M. Veerachary, F. Toriumi, N. Fujii, and H. Ko, "Maximum power point tracking of multiple photovoltaic arrays: A PSO approach," *IEEE Trans. Aerosp. Electron. Syst.*, vol. 47, no. 1, pp. 367–380, Jan. 2011.
[35] C. X. Liu and L. Q. Liu, "Particle swarm optimization MPPT method for PV materials in partial shading," *Adv. Mater. Res.*, vol. 321, pp. 72–75, Aug. 2011.
[36] M. A. Abdullah, A. H. M. Yatim, C. Tan, and A. Samosir, "Particle swarm optimization-based maximum power point tracking algorithm for wind energy conversion system," in *Proc. IEEE Int. Conf. Power Energy (PECon)*, Dec. 2012, pp. 65–70.
[37] J. Kennedy and R. Eberhart, "Particle swarm optimization," in *Proc. IEEE Int. Conf. Neural Netw.*, vol. 4, Nov./Dec. 1995, pp. 1942–1948.
[38] O. Kaiwartya, S. Kumar, D. K. Lobiyal, P. K. Tiwari, A. H. Abdullah, and A. N. Hassan, "Multiobjective dynamic vehicle routing problem and time seed based solution using particle swarm optimization," *J. Sensors*, vol. 2015, Dec. 2015, Art. no. 189832.
[39] N. A. Kamarzaman and C. W. Tan, "A comprehensive review of maximum power point tracking algorithms for photovoltaic systems," *Renew. Sustain. Energy Rev.*, vol. 37, pp. 585–598, Sep. 2014.
[40] O. Kaiwartya and S. Kumar, "Geocasting in vehicular adhoc networks using particle swarm optimization," in *Proc. Int. Conf. Inf. Syst. Design Commun.*, 2014, pp. 62–66.
[41] Z. M. Dalala, Z. U. Zahid, W. Yu, Y. Cho, and J.-S. Lai, "Design and analysis of an MPPT technique for small-scale wind energy conversion systems," *IEEE Trans. Energy Convers.*, vol. 28, no. 3, pp. 756–767, Sep. 2013.

MAJID ABDULLATEEF ABDULLAH received the B.Sc. degree in electrical power engineering from Al-Balqa' Applied University, Amman, Jordan, in 2006, the M.Sc. degree in electrical power and control from the Jordan University of Science and Technology, Irbid, Jordan, in 2009, and the Ph.D. degree in electrical power engineering from Universiti Teknologi Malaysia, Johor Bahru, Malaysia, in 2015. His research interests include renewable energy, power electronics converters, energy storage, and integrating energy storage with renewable energy systems.

TAWFIK AL-HADHRAMI received the M.Sc. degree in IT/applied system engineering from Heriot-Watt University, Edinburgh, U.K., and the Ph.D. degree in wireless mesh communication from the University of the West of Scotland, Glasgow, U.K., in 2015. He was involved in research at the Networking Group, University of the West of Scotland. He is currently a Lecturer at Nottingham Trent University (NTU), U.K. His research interests include Internet of Things and applications, network infrastructures and emerging technologies, artificial intelligence, Computational Intelligence and Applications Research Group. He is a member of the Network Infrastructure and Cyber Security Group, NTU. He was with different projects in industry and academia. He is involved in different projects with industries.

CHEE WEI TAN (M'11–SM'17) received the B.Eng. degree (Hons.) in electrical engineering from Universiti Teknologi Malaysia in 2003 and the Ph.D. degree in electrical engineering from Imperial College London, London, U.K., in 2008. He is a Senior Lecturer with Universiti Teknologi Malaysia and a member of the Power Electronics and Drives Research Group, Faculty of Engineering, School of Electrical Engineering. His research interests include the application of power electronics in renewable/alternative energy systems and the control of power electronics and energy management system in microgrids. He is also a Chartered Engineer registered with Engineering Council, U.K., and a Professional Engineer registered with the Board of Engineers Malaysia.

ABDUL HALIM YATIM (M'89–SM'01) received the B.Sc. degree in electrical and electronic engineering from Portsmouth Polytechnic, Portsmouth, U.K., in 1981, and the M.Sc. and Ph.D. degrees in power electronics from Bradford University, Bradford, U.K., in 1984 and 1990, respectively. Since 1981, he has been a member of the Faculty of Electrical Engineering, Universiti Teknologi Malaysia, and is currently a Professor and was the Dean of the Faculty from 2010 to 2012. He was a Commonwealth Academic Fellow at Heriot Watt University, Edinburgh, U.K., from 1994 to 1995, and a Visiting Scholar at the Virginia Power Electronics Centre, Virginia Polytechnic Institute and State University, Blacksburg, VA, USA, in 1993. His research interests include renewable/ alternative energy, power-electronics applications, and drives.

Dr. Yatim is a fellow of the Institution of Engineers Malaysia and a Registered Professional Engineer with the Malaysian Board of Engineers. He was the first Chapter Chairman of the Malaysian Section of the IEEE Industrial Electronics/Industry Applications/Power Electronics joint societies formed in 2003.

• • •

AUTHOR QUERIES

AUTHOR PLEASE ANSWER ALL QUERIES

PLEASE NOTE: We cannot accept new source files as corrections for your paper. If possible, please annotate the PDF proof we have sent you with your corrections and upload it via the Author Gateway. Alternatively, you may send us your corrections in list format. You may also upload revised graphics via the Author Gateway.

AQ:1 = Please provide the postal codes for "Taiz University, Universiti Teknologi Malaysia, and Nottingham Trent University."

AQ:2 = Author: Please confirm or add details for any funding or financial support for the research of this article.

AQ:3 = If you haven't done so already, please make sure you have submitted a graphical abstract for your paper. A Graphical Abstract is a figure that gives an overall summary of your paper (in addition to the abstract). Please choose a figure from the paper and supply a caption at your earliest convenience for the graphical abstract. Note that captions cannot exceed 1800 characters (including spaces). If you submitted a video as your graphical abstract, please make sure there is an overlay image and caption. Overlay images are usually a screenshot of your video that best represents the video. This is for readers who may not have access to video-viewing software. Please see an example in the link below: http://ieeeaccess.ieee.org/submitting-an-article/

AQ:4 = Please note that there were discrepancies between the accepted pdf [GE-Smart_cities.pdf] and the [ACCESS-ALHADHRAMI-2874525.doc] in the sentences on lines 55–60 and 160–170. We have followed [ACCESS-ALHADHRAMI-2874525.doc].

AQ:5 = Please confirm the volume no. for refs. [1] and [38].

AQ:6 = Please provide the volume no., issue no., page range, month, and year for ref. [6].

AQ:7 = Please note that references [13] and [25] are the same, hence we deleted Ref. [25] and renumbered the other references. This change will also reflect in the citations present in the body text. Please confirm.